Mutation Research xxx (2013) xxx–xxx

Contents lists available at ScienceDirect

Mutation Research/Fundamental and Molecular Mechanisms of Mutagenesis

journal homepage: www.elsevier.com/locate/molmut
Community address: www.elsevier.com/locate/mutres

Sequence-specific double strand breaks trigger P-TEFb-dependent Rpb1-CTD hyperphosphorylation

Giuliana Napolitano[a,1], Stefano Amente[a,1], Miriam Lubrano Lavadera[a], Giacomo Di Palo[a], Susanna Ambrosio[a], Luigi Lania[a], Gaetano Ivan Dellino[b], Pier Giuseppe Pelicci[b], Barbara Majello[a,*]

[a] Department of Biology, University of Naples 'Federico II', Naples, Italy
[b] Department of Experimental Oncology, European Institute of Oncology, Milan, Italy

ARTICLE INFO

Article history:
Received 13 March 2013
Received in revised form 2 July 2013
Accepted 17 July 2013
Available online xxx

Keywords:
Site-specific DSBs
AsiSI restriction enzyme
Rpb1-CTD
P-TEFb

ABSTRACT

Double strand DNA breaks (DSBs) are one of the most challenging forms of DNA damage which, if left unrepaired, can trigger cellular death and can contribute to cancer. A number of studies have been focused on DNA-damage response (DDR) mechanisms, and most of them rely on the induction of DSBs triggered by chemical compounds or radiations. However, genotoxic drugs and radiation treatments of cultured cell lines induce random DSBs throughout the genome, thus heterogeneously across the cell population, leading to variability of the cellular response. To overcome this aspect, we used here a recently described cell-based DSBs system whereby, upon induction of an inducible restriction enzyme, hundreds of site-specific DSBs are generated across the genome. We show here that sequence-specific DSBs are sufficient to activate the positive transcription elongation factor b (P-TEFb), to trigger hyperphosphorylation of the largest RNA polymerase II carboxyl-terminal-domain (Rpb1-CTD) and to induce activation of p53-transcriptional axis resulting in cell cycle arrest.

1. Introduction

DNA damage represents an impressive challenge to the integrity of genetic material and cells have evolved multifaceted mechanisms collectively termed the DNA damage response (DDR) to detect, sign and properly respond to various DNA injuries. DDR induces a global transcription reprogramming called transcriptional stress response (TSR) with the majority of genes being repressed. A subset of genes are activated in TSR, among them those whose activity is required to halt the cell cycle and repair the damage or eventually carry the cells toward apoptosis [1–5].

A common feature of cellular response to DNA damage induced by UV light, X-ray irradiation or different genotoxic drugs is hyperphosphorylation of CTD of the largest Rpb1 subunit of RNA polymerase II (Rpb1-CTD) [6,7]. Rpb1-CTD represents the docking site for a number of factors that, by interacting with and inducing its phosphorylation/dephosphorylation at Ser/Thr residues, regulate its activity as well as transcription progression along the gene unit and associated co-transcriptional events [8,9]. P-TEFb is one of the kinases that are involved in the regulation of RNA polymerase II (RNAPII) activity by phosphorylating the Rpb1-CTD tail during the transcriptional cycle. P-TEFb activity is regulated by a dynamic equilibrium between the small active complex (SC), made of CDK9/CyclinT1, and the large inactive complex (LC) where CDK9/CycT1 are associated to a snRNP complex made of 7SK snRNA, Hexim1, MeCPE and Larp7 [10–14]. The dynamic equilibrium between SC and LC P-TEFb complexes can be perturbed by transcriptional arrest, hypertrophic signals and by a variety of DNA-damaging agents that induce a rapid release of the P-TEFb LC complex with a concomitant accumulation of the active P-TEFb complex [15–21].

A number of studies have been focused on RNAPII transcription stalling in the presence of UV induced lesions, while the behavior of RNAPII when encounters a DSB lesion is a relative recent argument whose findings are still controversial, as recently discussed by Pankotai and Soutoglou [22 and references therein]. It has been suggested that the number and topology of the breaks may affect the molecular mechanisms mediating arrest of RNAPII [22–24]. Because the induction of DSBs triggered by chemical compounds or radiations of cultured cell lines causes random DSBs throughout the genome, several systems have been developed that rely on the use of restriction enzymes capable to generate unambiguously positioned sequence-specific DSBs, thus inducing a homogeneous, sequence specific, reproducible DNA damage [25–28]. Here we addressed whether sequence specific DSBs affect the

* Corresponding author. Tel.: +39 081 679062; fax: +39 081 679233.
E-mail address: majello@unina.it (B. Majello).
[1] These authors contributed equally to this work.

0027-5107/$ – see front matter © 2013 Elsevier B.V. All rights reserved.
http://dx.doi.org/10.1016/j.mrfmmm.2013.07.005

phosphorylation status of RNAPII and the relevant kinase involved in such effect. To this end we used the U2OS-derived cellular system (HA-AsiSI-ER, named AsiSI in the text) based on the activation of the inducible AsiSI restriction enzyme [28]. We found that site-specific DSBs trigger disruption of the P-TEFb LC complex leading to accumulation of active SC P-TEFb. Moreover, as consequence, we found hyperphosphorylation of Rpb1-CTD. In the same experimental conditions we also observed activation of the p53-dependent transcriptional pathway and cell cycle arrest.

2. Materials and methods

2.1. Cell culture and drug treatments

HA-AsiSI-ER-U2OS (AsiSI) and U2OS cells were cultured in Dulbecco's modified Eagle's medium (DMEM) supplemented with 10% fetal calf serum and 1 mg/ml puromycin at 37 °C in humidified atmosphere with 5% CO_2. Induction of HA-AsiSI-ER chimera was carried out as described in Iacovoni et al. [28] using 4-OHT (300 nM, from Sigma Aldrich). Doxorubicin (1 μM), camptothecin (12 μM) and nutlin-3 (10 μM) are from Sigma Aldrich. Flavopiridol (50 nM) was obtained from NIH AIDS research and Reference Reagent Program (Cat. #9925).

2.2. RNA interference

The following small interference RNA reagents (siRNAs) were purchased from Dharmacon: On Target Plus SMART pool targeting CDK9 (L-003243), On Target Plus non-target pool (D-001830-20).

AsiSI cells transfected with 100 nM siRNA targeting CDK9 or with scramble, non-targeting siRNA pool using MicroPorator Digital Bio Technology, a pipette-type electroporation system (Seoul, Korea). siRNAs were introduced into each 3×10^6 dissociated cells in 100 μl volume according to manufacturer's instructions (1230 V, 10 width, 4 pulses) and seeded in 100 mm culture dishes as previously reported [29]. After 48 h, cells were treated for 8 h with 4-OHT or vehicle (NT). After the treatments, cells were collected and extracts prepared as described in next paragraph.

2.3. Glycerol gradient, co-immunoprecipitation and immunoblotting

Whole-cell extracts were obtained using buffer A [11]. For glycerol gradient, protein extracts were ultracentrifuged at 40,000 rpm for 16 h at 4 °C in SW40.1 rotor on a pre-formed 5–45% discontinuous glycerol gradient containing buffer A. Samples were collected in 10 fractions (1 ml each starting from the top), and 20 μl of each fraction were separated by SDS-PAGE and analyzed by western blotting using appropriate antibodies.

Co-immunoprecipitation analyses were performed using whole-cell extracts (1 mg) incubated with the anti-Cyclin T1 (sc-10750) antibody. After extensive washes the recovered beads were resuspended in Laemmli buffer, resolved on SDS-PAGE and analyzed by western blotting.

The following antibodies were used: mouse monoclonal anti-8WG16 (MMS 126R) and mouse monoclonal anti-H5 (MMS 129R) from Covance, Inc.; rabbit polyclonal anti-Cdk9 (sc 8338), goat polyclonal anti-Cyclin T1 (sc-8127), mouse monoclonal anti-p53 (sc-126), rabbit polyclonal anti-p21 (sc-397), mouse monoclonal anti-actinin (sc-17829), mouse monoclonal anti-Cyclin B1 (sc-215) and rabbit polyclonal anti-Cyclin T1 (sc-10750) from Santa Cruz Biotechnology, Inc., Santa Cruz, CA; mouse monoclonal anti-P-p53 Ser15 (9286) from Cell Signaling Technology, Inc.; the rabbit polyclonal anti-Hexim1 (C4) was already described [30]. Binding was visualized by enhanced chemiluminescence (ECL-plus Kit, Amersham Biosciences).

2.4. Immunofluorescence and co-localization assays

Cells at the density of 5×10^4 were grown on coverslips in 2.5 cm dishes. Immunofluorescence was carried out as previously described [31]. Briefly, for immunofluorescence, U2OS cells were fixed and stained with rabbit anti-γH2AX (Cell Signaling Technology Inc.) for 30′ at 37 °C after brief permeabilization (0,1% Triton X-100/PBS) and pre-blocking (2% BSA-3% NRS) steps. After extensive washes, anti-rabbit-Cy3 secondary antibody has been used at the dilution of 1:400 for 30′ at room temperature. For co-localization analyses, after fixation and pre-blocking (2%BSA–3%NS), AsiSI cells were stained with both rabbit anti-γH2AX and mouse anti-HA (Invitrogen Corporation) for 30 min at 37 °C. Anti-mouse-Cy3 and anti-rabbit-FITC (Jackson Immunotech, West Grove, PA) secondary antibodies have been used after washes to detect mouse anti-HA and rabbit anti-γH2AX respectively. Nuclei were stained with DAPI (Invitrogen Corporation). Images were acquired using a Nikon Eclipse TE 2000-U microscope and digitally processed using Adobe Photoshop CS4 software.

2.5. qRT-PCR

cDNA was prepared from total RNA (1 mg) with Quantitec Reverse Transcription Kit (Qiagen) according to manufacturer's protocol. cDNA of each sample was prepared in triplicate and normalized to the expression of the housekeeping beta-glucoronidase (GUS) as previously described [18,19]. Quantitative analyses were performed using SYBR GREEN 2X PCR Master Mix (Applied Biosystems). Reactions were run in the AbiPrism 7900 HT sequence detector system (Perkin-Elmer Applied Biosystems). All values represent the average of at least three independent experiments. DNA sequences of the oligos used in this work are available upon request.

2.6. FACS analyses

For monoparametric DNA profile cells were treated as indicated in the text, collected by centrifugation and washed in phosphate-buffered saline (PBS). Cells were resuspended in hypotonic solution 0.1%Na-Citrate, 50 μg/ml propidium iodide, 50 μg/ml RNAse, and 0.00125% Nonidet P40, incubated in absence of light for 30′ at room temperature and diluted at the final concentration of 1×10^5 cells/ml.

Biparametric BrdU/DNA analysis: cells were treated as already described [32]. Briefly, after a 20 min pulse with 10 μM 5-bromo-2-deoxyuridine (BrdU, from Sigma Aldrich), culture medium was changed and cells were treated as indicated in the text. After treatments, cells were fixed with ice-cold ethanol, washed with PBS/1% BSA and subjected to a denaturation step with 2 N HCl for 25 min at room temperature. Denaturation was stopped with 0.1 M $Na_2B_4O_7$. After washes with PBS/1% BSA, cells were incubated with anti-BrdU (cat. No. 347580, Becton Dickinson) in PBS/1% BSA. After incubation with the secondary anti-mouse FITC (F2883, Sigma Aldrich) cells were washed and incubated in absence of light overnight with PI (2.5 μg/ml) and RNAse (50 μg/ml). Cytofluorimetric acquisitions and analyses were performed on a Becton Dickinson FACScalibur flow cytometer using FACSDiva, CellQuest Pro and ModFit LT 3.0 softwares.

3. Results and discussion

3.1. AsiSI induced DSBs trigger P-TEFb-dependent Rpb1-CTD hyperphosphorylation

A common feature of the cellular response to UV radiations and drug-induced DNA damage is the induction of a high phosphorylation degree of the Rpb1-CTD [6,7,33]. The CTD tail of Rpb1 serves as a scaffold for the interaction of a wide range of factors that orchestrate transcription and co-transcriptional processes, and it has been suggested that the hyper-phosphorylated status of the CTD represents a signal for rapid Rpb1 proteasomal degradation [34–36].

However, in-depth understanding of the functional consequences of hyper-phosphorylation triggered by diverse DNA damaging agents has been hampered because most DNA damaging agents act non-selectively throughout the genome, generating a heterogeneous genotoxic response. Here we used an inducible restriction enzyme cellular system whereby hundreds of DSBs are generated across the genome. AsiSI cells express the 8 bp restriction enzyme AsiSI fused to HA epitope and to a modified estrogen receptor ligand binding domain that induces nuclear localization of the enzyme only after 4-OHT administration to cells [28].

As shown in Fig. 1A, we observed nuclear accumulation of HA-AsiSI-ER chimera by immunofluorescence analysis of AsiSI cells treated with 4-OHT for increasing time, and we detected appearance of γ-H2AX foci after 0.5 h following drug administration.

Then we tested CTD-Rpb1 phosphorylation status following DSBs generation. Western blots analyses showed that CTD hyperphosphorylation takes place after 2 h of 4-OHT treatments (Fig. 1B). Using 8WG16 antibody that recognizes the unphosphorylated heptapeptides of the CTD thus detecting total Rpb1 (that is, all isoforms), we observed accumulation of the slower IIo band (mostly hyper-phosphorylated) and a concomitant decrease of the faster hypo-phosphorylated IIa form of Rpb1. The hyper-phosphorylation of Rpb1-CTD increased during time of treatment as documented by the ratio between the hyper-phosphorylated IIo and hypo-phosphorylated IIa forms of CTD. We included in our experiments treatment with Camptothecin (CPT) that is known to induce DSBs [37]. CTD hyper-phosphorylation was also assayed using the anti-H5 antibody that mainly recognizes the phospho-Ser2-CTD.

Please cite this article in press as: G. Napolitano, et al., Sequence-specific double strand breaks trigger P-TEFb-dependent Rpb1-CTD hyperphosphorylation, Mutat. Res.: Fundam. Mol. Mech. Mutagen. (2013), http://dx.doi.org/10.1016/j.mrfmmm.2013.07.005

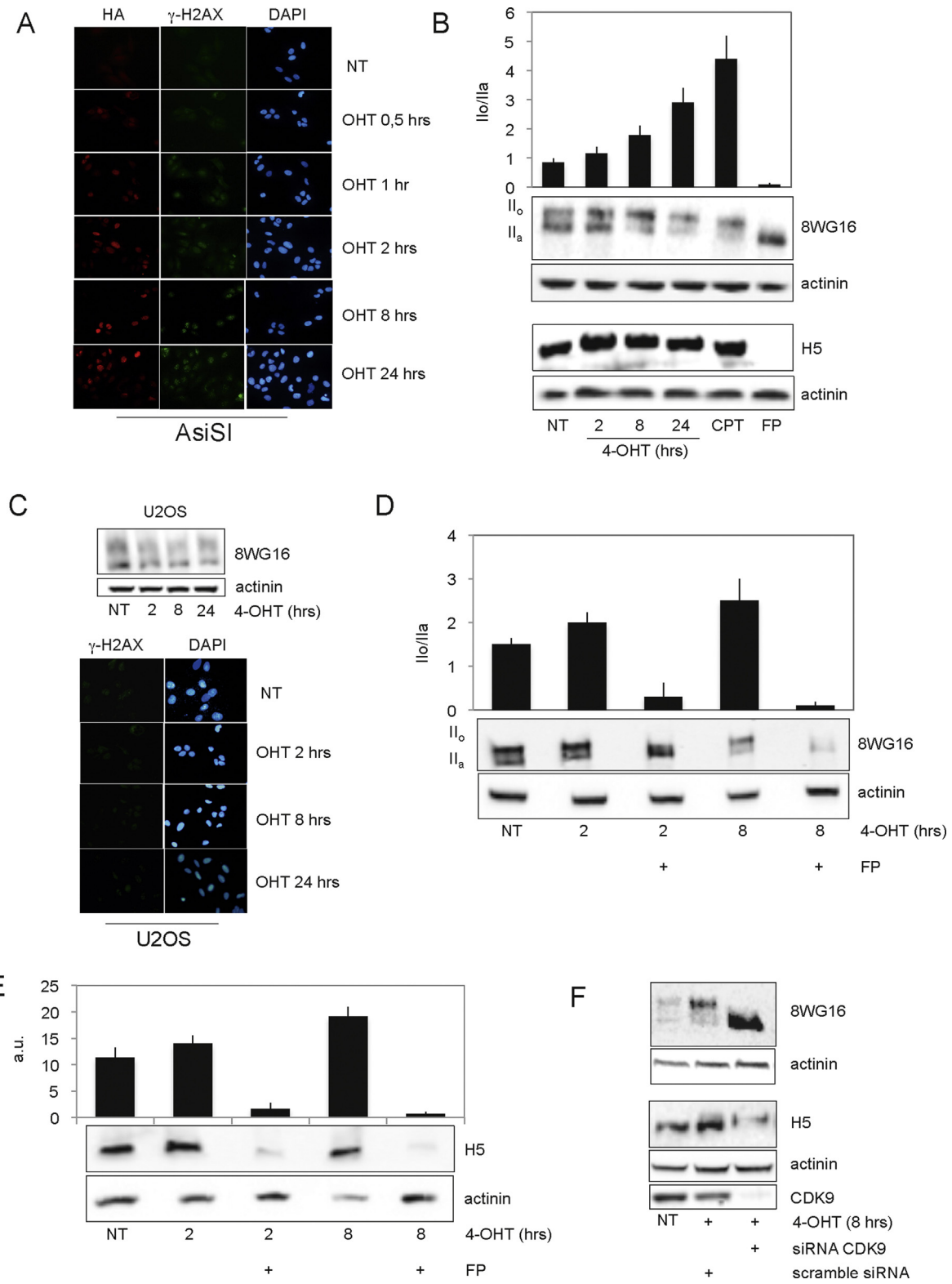

Fig. 1. DBSs determine hyper-phosphorylation of Rpb1 carboxyl-terminal domain that is dependent on P-TEFb activity. (A) AsiSI cells were treated with 4-OHT or vehicle (NT) for the indicated time. Fixed cells were stained with anti-HA and anti-γH2AX antibodies to evaluate nuclear accumulation of the HA-AsiSI-ER chimera and the presence of DSBs respectively by immunofluorescence assay. DAPI staining of nuclei is shown. (B) AsiSI cells were treated with 4-OHT for the indicated time, with camptothecin (CPT) for three hours or with vehicle (NT) as indicated. Cellular extracts were prepared and probed with anti-8WG16 and anti-H5 antibodies. Histogram bars show the ratio between II_o and II_a forms of Rpb1-CTD. Standard deviation bars are shown. (C) Upper panel: U2OS cells were treated with 4-OHT or vehicle (NT) for the indicated time. Total cellular extracts were prepared and stained with anti-8WG16. Lower panel: U2OS cells were treated as in (C) upper panel. After fixation cells were stained with anti-γH2AX. Nuclei were stained with DAPI. (D) AsiSI cells were treated with vehicle (NT), 4-OHT alone or in combination with the P-TEFb inhibitor FP as indicated. Cellular extracts were probed with anti-8WG16 antibody. The ratio between Rpb1-II_o and Rpb1-II_a is shown in the upper histogram panel together with standard deviation bars. (E) AsiSI cells were treated as in (D). Extracts were probed with anti-H5 antibody that recognizes the P-Ser2 of CTD heptads in Rpb1. Values shown in histograms are the average of 2–3 different biological experiments, and the values have been calculated as fold changes to the untreated sample (set to one). (F) AsiSI cells were transfected with siRNA for CDK9 or with scramble siRNA as indicated. After 48 h, cells were treated with 4-OHT (or vehicle, NT) for 8 h and collected. Extracts were prepared and RNAPII probed by WB with anti-8WG16 and anti-H5 antibodies. WB anti-CDK9 is shown to evaluate CDK9 silencing. Blots anti-actinin are shown as loading control.

Please cite this article in press as: G. Napolitano, et al., Sequence-specific double strand breaks trigger P-TEFb-dependent Rpb1-CTD hyperphosphorylation, Mutat. Res.: Fundam. Mol. Mech. Mutagen. (2013), http://dx.doi.org/10.1016/j.mrfmmm.2013.07.005

To exclude that 4-OHT treatment could directly affect Rpb1-CTD phosphorylation, we treated the parental U2OS cell line with 4-OHT and analyzed Rpb1-CTD phosphorylation as reported in Fig. 1C (upper panel); results showed no direct effect of 4-OHT in U2OS cells and confirmed that the hyper-phosphorylation of Rpb1-CTD in AsiSI cells is a consequence of sequence-specific DSBs. Moreover, we also assessed that 4-OHT administration to U2OS cells do not lead to γ-H2AX foci formation (Fig. 1C, lower panel).

The CTD domain of Rpb1 is a substrate of several kinases in vitro and in vivo. Notably, P-TEFb is the kinase responsible of Ser2 phosphorylation at the switch of transcription from initiation/pausing to processive elongation. We sought to determine whether P-TEFb might be the kinase responsible for the observed CTD hyper-phosphorylation following AsiSI-dependent DNA cuts and to this end we treated cells with 4-OHT alone or in combination with flavopiridol (FP). FP is considered a potent inhibitor of CDKs with significant selectivity for CDK9 as its IC50 has been found to be about 7 times lower than that of the closest CDK IC50 reported to date [38–40]. As shown in Fig. 1 panel D, the ratio between II_o and II_a Rpb1 forms sharply decreases following co-treatments of cells with 4-OHT and FP. These results were confirmed by probing the extracts with anti-H5 antibody that recognizes the P-Ser2-CTD (Fig. 1E). Albeit FP shows a high selectivity for CDK9, we cannot exclude that the observed effects could be also due to a concomitant FP inhibition of other cellular kinases. To further validate the role of CDK9 in the hyper-phosphorylation of Rpb1-CTD-(Ser2) following DSBs, we silenced CDK9 expression by using specific siRNAs. AsiSI were transfected with siRNAs targeting CDK9, as well as with scramble, non-targeting siRNAs for 48 h before treatment with 4-OHT. As shown in Fig. 1F, in cells silenced for CDK9 expression, 4-OHT-dependent CTD hyper-phosphorylation was impaired.

Collectively, these data showed that AsiSI-induced DSBs trigger hyper-phosphorylation of Rpb1-CTD at Ser2 and that P-TEFb is the kinase responsible for the most of the observed Rpb1-CTD-(Ser2) phosphorylation.

3.2. AsiSI-induced DSBs determine dissociation of the P-TEFb complex

It is known that initiation of transcriptional response following genotoxic stress induced by several DNA damaging agents causes a rapid release of P-TEFb from the inactive LC complex concurrent with Rpb1-CTD hyper-phosphorylation [17–19,33–36].

To investigate if AsiSI-dependent DNA damage determines P-TEFb dissociation, we analyzed the ratio between SC and LC forms of P-TEFb after treatment of cells with 4-OHT for different times by glycerol fractionation of cell lysates. Cellular lysates from AsiSI cells were ultracentrifuged on a glycerol gradient and the recovered fractions were analyzed by western blotting with anti-CDK9 and anti-HEXIM1 antibodies. As shown in Fig. 2A, treatment with 4-OHT shortly (1.5 h) determined dissociation of P-TEFb (compare NT and 4-OHT 1.5 h lanes 7–8, Fig. 2A) that remained constant until 4 h of treatment (4-OHT 4 h lanes 7–8, Fig. 2A). Since the dissociation is not complete, probably reflecting the slighter DNA damaging insult caused by AsiSI DSBs, we wished to further validate P-TEFb dissociation by co-immunoprecipitation analyses. Cyclin T1 associated proteins were immunoprecipitated in untreated, 4-OHT and control camptothecin (CPT) treated cells to investigate the presence of the CDK9 and Hexim1 proteins in the complex. As shown in Fig. 2B, dissociation of Hexim1 from the LC P-TEFb started at 2 h after treatment and increased at 4 h of 4-OHT treatment, to levels comparable to those obtained following CPT treatment. Collectively, these data demonstrated that sequence-specific DNA damage induced by AsiSI determines

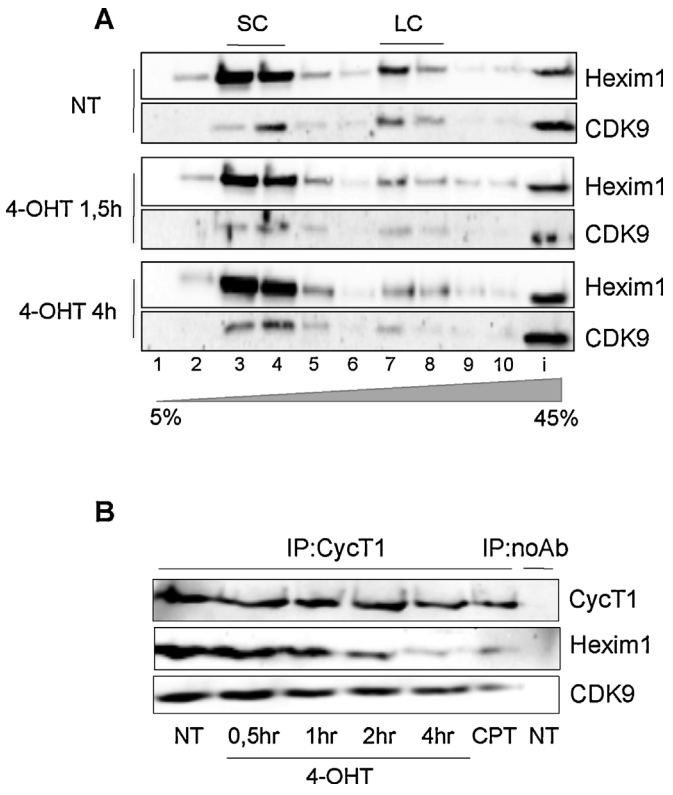

Fig. 2. AsiSI-dependent DBSs induce P-TEFb activation. (A) AsiSI cells were treated with 4-OHT or vehicle (NT) as indicated. Whole cell extract were prepared and separated on a discontinuous glycerol gradient (5–45%) by ultracentrifugation. Fractions were loaded on gel compared with input (i) and immunoblotted with anti-Hexim1 and anti-CDK9 to evaluate the extent of P-TEFb SC accumulation following DSBs. Immunoblots show that DSBs induced by AsiSI-dependent DNA cuts induce dissociation of P-TEFb large complex (LC) and the concomitant accumulation of the small complex (SC). (B) AsiSI cells were treated with vehicle (NT), 4-OHT for the indicated time and with CPT for three hours. 1 mg of the whole cell extract was immunoprecipitated with anti-CycT1 (IP:CycT1) or pre-immune serum (IP:no Ab). The immunoprecipitated materials were loaded on gel and probed with anti-CycT1, anti-Hexim1 and anti-CDK9 to evaluate Hexim1 dissociation from P-TEFb. Immunoblots show that 4-OHT determines Hexim1 dissociation from P-TEFb at the same extent of CPT treatment.

P-TEFb activation, which in turn is responsible for CTD-Ser2 hyper-phosphorylation (Figs. 1 and 2).

3.3. AsiSI-induced DSBs determine activation of the p53 transcriptional axis with a concomitant G2/M cell cycle arrest

DNA damage alters the global pattern of gene expression that orchestrates a variety of cellular mechanisms including DNA repair, growth arrest and/or apoptosis. Following DNA damage, p53 is phosphorylated and thus activated by ATM and ATR kinases, as well as by their substrates Chk1 and Chk2 [1,2]. The activated and stable p53 enhances the expression of several genes that cooperate to arrest cell cycle, as for example CDKN1A (p21) and GADD45a as well as to induce proapoptotic markers such as BBC3 (PUMA) and BAX.

Firstly, we determined whether AsiSI directed DNA breaks were sufficient to induce p53 and p21 gene expression. As shown in Fig. 3 (panel A), 4-OHT led to p53 accumulation, even though at lesser extent than drugs capable to induce genotoxicity and cellular stress (doxorubicin DXR, CPT, FP) or Nutlin-3, which disrupting p53-MDM2 interaction, releases the active form of p53 in the absence of DNA damage. According to these results, we also observed a concomitant increase of the p21 protein levels.

Please cite this article in press as: G. Napolitano, et al., Sequence-specific double strand breaks trigger P-TEFb-dependent Rpb1-CTD hyperphosphorylation, Mutat. Res.: Fundam. Mol. Mech. Mutagen. (2013), http://dx.doi.org/10.1016/j.mrfmmm.2013.07.005

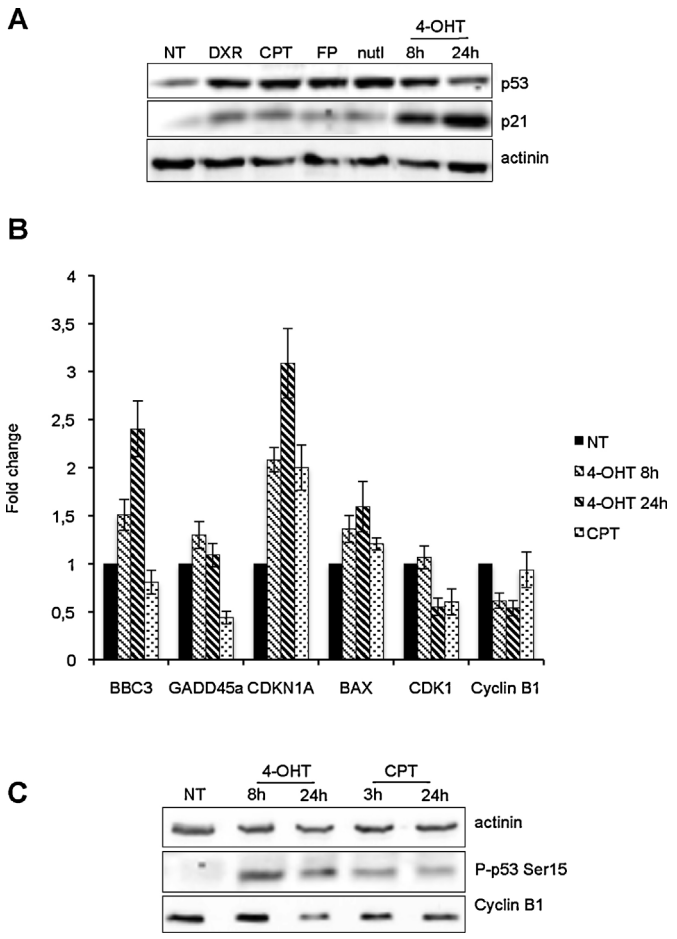

Fig. 3. AsiSI-induced DSBs determine activation of p53 target genes. (A) Whole cell extracts from AsiSI cells treated for three hours with vehicle (NT), doxorubicin (DXR), camptothecin (CPT), flavopiridol (FP), nutlin-3 (nutl) and with 4-OHT for the indicated time were prepared and probed with anti-p53 and anti-p21. p53 and p21 proteins accumulate in response to diverse DNA damaging agents or stress cell drugs. Actinin has been probed as a loading control. (B) AsiSI cells were treated with vehicle (NT), 4-OHT as indicated and CPT for three hours. Total mRNA was prepared and levels of BBC3, GADD45a, CDKN1A, BAX, CDK1 and Cyclin B1 mRNAs were quantified by qRT-PCR and normalized to GUS mRNA level. Standard deviation bars are indicated. (C) Whole cell extracts from AsiSI cells treated with vehicle (NT), CPT and 4-OHT for the indicated time were prepared, separated on gel and probed with anti-P-p53-Ser15 and anti-Cyclin B1. Actinin has been probed as a loading control. Immunoblots show that phosphorylation of p53(Ser15) takes place following 4-OHT and CPT treatments.

Assuming by these findings the activation of the p53-dependent transcriptional pathway, we analyzed the expression levels of dedicated p53 gene targets as CDKN1A, BBC3, GADD45a and BAX by qRT-PCR. Our data show that site-specific DSBs induced by the AsiSI activity caused up-regulation of the p53-dependent analyzed genes (Fig. 3B). Accordingly, CPT treatments also led to accumulation of CDKN1A and BAX, while BBC3 resulted unaffected and GADD45a downregulated. GADD45a down-regulation in presence of p53 over-expression is in agreement to published data [41]. Regarding BBC3, we speculate that the differences in BBC3 mRNA levels after treatments with CTP and 4-OHT are likely dependent on the specific cellular system used: it is reported that in the U2OS parental cell line, BBC3 overexpression following cisplatin administration is missing because of high presence of miR221-222 that directly targets BBC3 mRNA [42,43].

Since it is known that following UV-dependent DNA damage, Cyclin B1 and its kinase partner CDK1 are down-regulated due to reduction of GCN5 association to their respective promoter regions [44,45], we also looked at their expression. As shown in Fig. 3B, we observed reduction of Cyclin B1 and CDK1 expression following 4-OHT treatment.

We also analyzed p53-(Ser15) phosphorylation status and Cyclin B1 protein levels by comparing the effect of AsiSI-dependent DSBs to CPT treatment. As shown in Fig. 3C we observed increasing amount of phosphorylated p53 following 4-OHT treatment and CPT, and a relative small reduction of Cyclin B1 protein levels at 24 h after 4-OHT treatment.

To monitor cell cycle distribution upon induction of DSBs induced by AsiSI site-specific cuts, we performed monoparametric FACS analyses of propidium-stained cells upon drug administration and compared the results to those obtained by treatment with CPT. As shown in Fig. 4A, while cells treated with CPT arrested in G1, with cells in G1 phase increasing from 36% to 50% after drug administration, on sharp contrast, AsiSI-dependent DSBs determined G2/M arrest, with G2/M cells increasing from 16% to 46% following 4-OHT treatment. Our data are in agreement with previous report by the Legube group [46]; besides, we show that cell cycle arrest at G2/M is already evident after 8 h of treatment with 4-OHT.

We also performed a bromodeoxyuridine/DNA (BrdU/DNA) biparametric flow cytometric analysis to obtain a distinct evaluation of cell cycle perturbations of cells that are in S phase (BrdU-positive cells) or in G1 or in G2/M (BrdU-negative cells) after AsiSI-induced DNA breaks [32].

Fig. 4B shows the biparametric BrdU/DNA analysis on the AsiSI cells following 4-OHT treatments for different times. As shown, G2/M arrest was evident after 8 h of treatment (compare 4-OHT 8 h to growing $t = 8$ h). Moreover, after 24 h of treatment the majority of cells were blocked in G2/M (compare 4-OHT 24 h to growing $t = 24$); among these cells a population of cells that was in G1 started a new DNA synthesis cycle although remaining halted in G2/M (BrdU positive cells). In fact, G2/M BrdU-positive cells increased from 6% to 30%, thus confirming the results obtained with monoparametric DNA profile analysis (Fig. 4A and B).

Data presented here showed that DSBs induced by AsiSI activity determine down-regulation of Cyclin B1/CDK1 and the concomitant block of cell cycle in G2/M. The activated Cyclin B1/CDK1 complex exerts its role in promoting cells mitosis. In the presence of DSBs, it has been shown that p21 binds Cyclin B1/CDK1 to block its activity by nuclear retention [47,48]. We speculate that the inhibition of Cyclin B1/CDK1 induced by AsiSI activity mimics the p21-mediated inhibition of the complex, thus halting cells in G2/M. However, further experiments could address this point.

Collectively, our results indicate that, in the inducible cellular system AsiSI the limited amount of breaks induced by the AsiSI enzyme is sufficient for the repartitioning of P-TEFb in the active SC; moreover, we suggest that the active CDK9 is responsible for induction of hyperphosphorylation of Rpb1-CTD in this system. We found that site-specific DSBs trigger the activation of genes that take part in TSR, namely p53, CDKN1A (p21), BBC3 (PUMA), GADD45a and BAX similarly to classical non site-specific inducers of DSBs. In contrast to the G1 arrest that follows CPT-mediated damage, in this cellular model we observed arrest in G2/M as consequence of AsiSI-induced DSBs.

Although we cannot exclude a variability of AsiSI enzyme efficiency among cells due to chromatin structure and accessibility, which could lead to a minor level of heterogeneity in the produced DNA cuts [28], our data establish that the use of an inducible enzyme-based DNA damage cellular system may provide a useful experimental system not only for an in-depth understanding of chromatin dynamic involved in DSBs recognition, signaling and repair, but also in the genetic transcriptional reprogramming that follows DNA damage.

Please cite this article in press as: G. Napolitano, et al., Sequence-specific double strand breaks trigger P-TEFb-dependent Rpb1-CTD hyperphosphorylation, Mutat. Res.: Fundam. Mol. Mech. Mutagen. (2013), http://dx.doi.org/10.1016/j.mrfmmm.2013.07.005

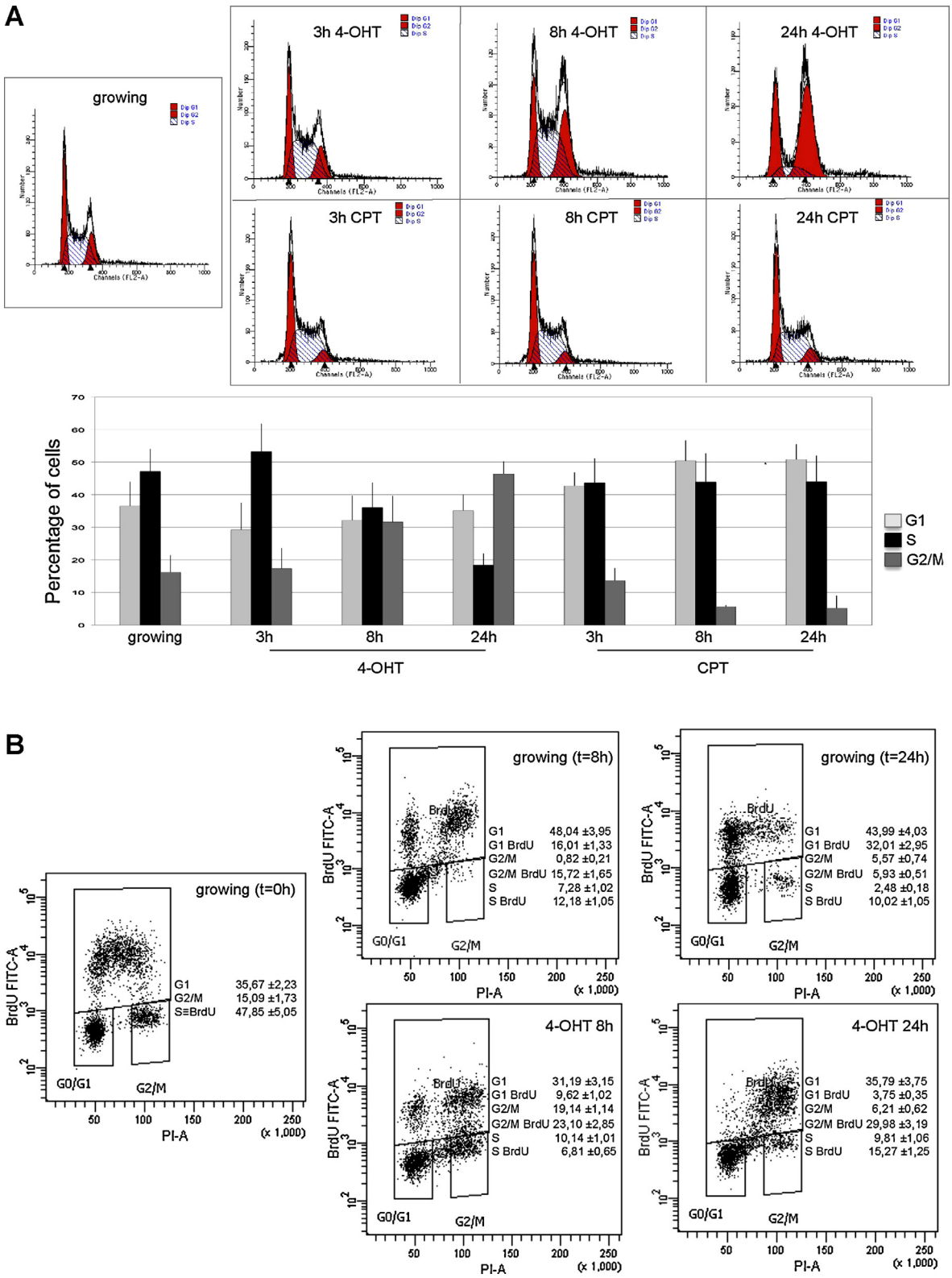

Fig. 4. Site-specific DSBs induced by AsiSI lead to G2/M arrest. (A) AsiSI cells were treated with vehicle (growing), 4-OHT or CPT as indicated. Cells were prepared and stained with propidium iodide to analyze their DNA profile by FACS analysis. Data have been reported in histogram graphs. Histograms of DNA profiles of analyzed cells are also shown. Data are from at least three independent assays. Images are from representative experiments. 4-OHT administration halts cells in G2/M while CPT induces an arrest in G1/S phase of cell cycle. (B) Biparametric BrdU/DNA analysis of cells treated with vehicle (growing, upper panels) compared to cells treated with 4-OHT for the indicated times (4-OHT 8 h and 24 h, lower panels). Cells were firstly subjected to 20 min BrdU pulse and then treated as indicated. After fixation, cells were stained with both propidium iodide and anti-BrdU and were successively analyzed by flow cytometry. BrdU positive cells marked the DNA replicating fraction at the time of treatments, thus allowing us to monitor the effects of the genotoxic insult in relation to cell cycle phase. As time goes on, both BrdU positive and negative cells progressed through the cell cycle and the calculated fractions were reported in each dotplot. In particular, G1 BrdU fraction represent cells initially in S phase entering a new cell cycle: part of these cells initially completed a first round of cell division (G1 BrdU at 8 h) to be stopped in G2/M after an additional DNA replication phase. Images are from representative experiments. Sequence-specific DSBs arising from AsiSI activity lead to accumulation of cells in G2/M.

Please cite this article in press as: G. Napolitano, et al., Sequence-specific double strand breaks trigger P-TEFb-dependent Rpb1-CTD hyperphosphorylation, Mutat. Res.: Fundam. Mol. Mech. Mutagen. (2013), http://dx.doi.org/10.1016/j.mrfmmm.2013.07.005

Conflict of interest statement

The authors declare no conflict of interest.

Acknowledgements

We thank G. Legube for providing the HA-AsiSI-ER cells. We thank M. Faretta for helpful discussions. This work was supported by grants from AIRC and MIUR.

References

[1] J.W. Harper, S.J. Elledge, The DNA damage response: ten years after, Mol. Cell 28 (2007) 739–745.
[2] S.P. Jackson, J. Bartek, The DNA-damage response in human biology and disease, Nature 461 (2009) 1071–1078.
[3] D.A. Rockx, R. Mason, A. van Hoffen, M.C. Barton, E. Citterio, D.B. Bregman, A.A. van Zeeland, H. Vrieling, L.H. Mullenders, UV-induced inhibition of transcription involves repression of transcription initiation and phosphorylation of RNA polymerase II, Proc. Natl. Acad. Sci. U. S. A. 97 (2000) 10503–10508.
[4] M. Gentile, L. Latonen, M. Laiho, Cell cycle arrest and apoptosis provoked by UV radiation-induced DNA damage are transcriptionally highly divergent responses, Nucleic Acids Res. 31 (2003) 4779–4790.
[5] L. Proietti-De-Santis, P. Drane, J.M. Egly, Cockayne syndrome B protein regulates the transcriptional program after UV irradiation, EMBO J. 25 (2006) 1915–1923.
[6] Z. Luo, J. Zheng, Y. Lu, D.B. Bregman, Ultraviolet radiation alters the phosphorylation of RNA polymerase II large subunit and accelerates its proteasome-dependent degradation, Mutat. Res. 486 (2001) 259–274.
[7] B.P. Somesh, J. Reid, W.F. Liu, T.M. Sogaard, H. Erdjument-Bromage, P. Tempst, J.Q. Svejstrup, Multiple mechanisms confining RNA polymerase II ubiquitylation to polymerases undergoing transcriptional arrest, Cell 121 (2005) 913–923.
[8] B. Bartkowiak, A.L. Mackellar, A.L. Greenleaf, Updating the CTD story: from tail to epic, Genet. Res. Int. 2011 (2011) 623718.
[9] J.Q. Svejstrup, Transcription: another mark in the tail, EMBO J. 31 (2012) 2753–2754.
[10] Z. Yang, Q. Zhu, K. Luo, Q. Zhou, The 7SK small nuclear RNA inhibits the CDK9/cyclin T1 kinase to control transcription, Nature 414 (2001) 317–322.
[11] V.T. Nguyen, T. Kiss, A.A. Michels, O. Bensaude, 7SK small nuclear RNA binds to and inhibits the activity of CDK9/cyclin T complexes, Nature 414 (2001) 322–325.
[12] A.A. Michels, A. Fraldi, Q. Li, T.E. Adamson, F. Bonnet, V.T. Nguyen, S.C. Sedore, J.P. Price, D.H. Price, L. Lania, O. Bensaude, Binding of the 7SK snRNA turns the HEXIM1 protein into a P-TEFb (CDK9/cyclin T) inhibitor, EMBO J. 23 (2004) 2608–2619.
[13] C. Jeronimo, D. Forget, A. Bouchard, Q. Li, G. Chua, C. Poitras, C. Therien, D. Bergeron, S. Bourassa, J. Greenblatt, B. Chabot, G.G. Poirier, T.R. Hughes, M. Blanchette, D.H. Price, B. Coulombe, Systematic analysis of the protein interaction network for the human transcription machinery reveals the identity of the 7SK capping enzyme, Mol. Cell 27 (2007) 262–274.
[14] B.J. Krueger, C. Jeronimo, B.B. Roy, A. Bouchard, C. Barrandon, S.A. Byers, C.E. Searcey, J.J. Cooper, O. Bensaude, E.A. Cohen, B. Coulombe, D.H. Price, LARP7 is a stable component of the 7SK snRNP while P-TEFb, HEXIM1 and hnRNP A1 are reversibly associated, Nucleic Acids Res. 36 (2008) 2219–2229.
[15] M. Sano, M. Abdellatif, H. Oh, M. Xie, L. Bagella, A. Giordano, L.H. Michael, F.J. DeMayo, M.D. Schneider, Activation and function of cyclin T-Cdk9 (positive transcription elongation factor-b) in cardiac muscle-cell hypertrophy, Nat. Med. 8 (2002) 1310–1317.
[16] C. Barrandon, F. Bonnet, V.T. Nguyen, V. Labas, O. Bensaude, The transcription-dependent dissociation of P-TEFb-HEXIM1-7SK RNA relies upon formation of hnRNP-7SK RNA complexes, Mol. Cell. Biol. 27 (2007) 6996–7006.
[17] G. Napolitano, F. Varrone, B. Majello, L. Lania, Activation of P-TEFb induces p21 leading to cell cycle arrest, Cell Cycle 6 (2007) 1126–1129.
[18] G. Napolitano, S. Amente, V. Castiglia, B. Gargano, V. Ruda, X. Darzacq, O. Bensaude, B. Majello, L. Lania, Caffeine prevents transcription inhibition and P-TEFb/7SK dissociation following UV-induced DNA damage, PLoS ONE 5 (2010) e11245.
[19] S. Amente, B. Gargano, G. Napolitano, L. Lania, B. Majello, Camptothecin releases P-TEFb from the inactive 7SK snRNP complex, Cell Cycle 8 (2009) 1249–1255.
[20] N. He, A.C. Pezda, Q. Zhou, Modulation of a P-TEFb functional equilibrium for the global control of cell growth and differentiation, Mol. Cell. Biol. 26 (2006) 7068–7076.
[21] X. Contreras, M. Barboric, T. Lenasi, B.M. Peterlin, HMBA releases P-TEFb from HEXIM1 and 7SK snRNA via PI3K/Akt and activates HIV transcription, PLoS Pathog. 3 (2007) 1459–1469.
[22] T. Pankotai, E. Soutoglou, Double strand breaks hurdles for RNA polymerase II transcription? Transcription 4 (2013) 34–38.
[23] N.M. Shanbhag, I.U. Rafalska-Metcalf, C. Balane-Bolivar, S.M. Janicki, R.A. Greenberg, ATM-dependent chromatin changes silence transcription in cis to DNA double-strand breaks, Cell 141 (2010) 970–981.
[24] T. Pankotai, C. Bonhomme, D. Chen, E. Soutoglou, DNAPKcs-dependent arrest of RNA polymerase II transcription in the presence of DNA breaks, Nat. Struct. Mol. Biol. 19 (2012) 276–282.
[25] P. Rouet, F. Smih, M. Jasin, Expression of a site-specific endonuclease stimulates homologous recombination in mammalian cells, Proc. Natl. Acad. Sci. U. S. A. 91 (1994) 6064–6068.
[26] M. Jasin, Genetic manipulation of genomes with rare-cutting endonucleases, Trends Genet. 12 (1996) 224–228.
[27] E. Berkovich, R.J. Monnat Jr., M.B. Kastan, Roles of ATM and NBS1 in chromatin structure modulation and DNA double-strand break repair, Nat. Cell Biol. 9 (2007) 683–690.
[28] J.S. Iacovoni, P. Caron, I. Lassadi, E. Nicolas, L. Massip, D. Trouche, G. Legube, High-resolution profiling of gammaH2AX around DNA double strand breaks in the mammalian genome, EMBO J. 29 (2010) 1446–1457.
[29] S. Amente, A. Bertoni, A. Morano, L. Lania, E.V. Avvedimento, B. Maljello, LSD1-mediated demethylation of histone H3 lysine 4 triggers Myc-induced transcription, Oncogene 29 (2010) 3691–3702.
[30] A.A. Michels, V.T. Nguyen, A. Fraldi, V. Labas, M. Edwards, F. Bonnet, L. Lania, O. Bensaude, MAQ1 and 7SK RNA interact with CDK9/cyclin T complexes in a transcription-dependent manner, Mol. Cell. Biol. 23 (2003) 4859–4869.
[31] G. Napolitano, P. Licciardo, R. Carbone, B. Majello, L. Lania, CDK9 has the intrinsic property to shuttle between nucleus and cytoplasm, and enhanced expression of cyclin T1 promotes its nuclear localization, J. Cell. Physiol. 192 (2002) 209–215.
[32] E. Erba, D. Bergamaschi, L. Bassano, G. Damia, S. Ronzoni, G.T. Faircloth, M. D'Incalci, Ecteinascidin-743 (ET-743), a natural marine compound, with a unique mechanism of action, Eur. J. Cancer 37 (2001) 97–105.
[33] H.P. Phatnani, A.L. Greenleaf, Phosphorylation and functions of the RNA polymerase II CTD, Genes Dev. 20 (2006) 2922–2936.
[34] G.F. Heine, A.A. Horwitz, J.D. Parvin, Multiple mechanisms contribute to inhibit transcription in response to DNA damage, J. Biol. Chem. 283 (2008) 9555–9561.
[35] K.B. Lee, D. Wang, S.J. Lippard, P.A. Sharp, Transcription-coupled and DNA damage-dependent ubiquitination of RNA polymerase II in vitro, Proc. Natl. Acad. Sci. U. S. A. 99 (2002) 4239–4244.
[36] N. Inukai, Y. Yamaguchi, I. Kuraoka, T. Yamada, S. Kamijo, J. Kato, K. Tanaka, H. Handa, A novel hydrogen peroxide-induced phosphorylation and ubiquitination pathway leading to RNA polymerase II proteolysis, J. Biol. Chem. 279 (2004) 8190–8195.
[37] Y. Pommier, Topoisomerase I inhibitors: camptothecins and beyond, Nat. Rev. Cancer 6 (2006) 789–802.
[38] S.H. Chao, K. Fujinaga, J.E. Marion, R. Taube, E.A. Sausville, A.M. Senderowicz, B.M. Peterlin, D.H. Price, Flavopiridol inhibits P-TEFb and blocks HIV-1 replication, J. Biol. Chem. 275 (2000) 28345–28358.
[39] B.A. Carlson, M.M. Dubay, E.A. Sausville, L. Brizuela, P.J. Worland, Flavopiridol induces G1 arrest with inhibition of cyclin-dependent kinase (CDK) 2 and CDK4 in human breast carcinoma cells, Cancer Res. 56 (1996) 2973–2978.
[40] A.M. Senderowicz, E.A. Sausville, Preclinical and clinical development of cyclin-dependent kinase modulators, J. Natl. Cancer Inst. 92 (2000) 376–387.
[41] G. Xiao, A. Chicas, M. Olivier, A DNA damage signal is required for p53 to activate gadd45, Cancer Res. 60 (2000) 1711–1719.
[42] J.A. Freeman, J. Espinosa, The impact of post-transcriptional regulation in the p53 network, Brief. Funct. Genomics 12 (2013) 46–57.
[43] G. Zhao, C. Cai, T. Yang, X. Qiu, B. Liao, W. Li, Z. Ji, J. Zhao, H. Zhao, M. Guo, Q. Ma, C. Xiao, Q. Fan, B. Ma, MicroRNA-221 induces cell survival and cisplatin resistance through PI3K/Akt pathway in human osteosarcoma, PLoS ONE 8 (2013) e53906.
[44] M. Shimada, H. Niida, D.H. Zineldeen, H. Tagami, M. Tanaka, H. Saito, M. Nakanishi, Chk1 is a histone H3 threoinine 11 kinase that regulates DNA damage-induced transcriptional repression, Cell 132 (2008) 221–232.
[45] J.V. Tjeertes, K.M. Miller, S.P. Jackson, Screen for DNA-damage-responsive histone modifications identifies H3K9Ac and H3K56Ac in human cells, EMBO J. 28 (2009) 1878–1889.
[46] L. Massip, P. Caron, J.S. Iacovoni, D. Trouche, G. Legube, Deciphering the landscape induced around DNA double strand breaks, Cell Cycle 9 (2010) 2963–2972.
[47] F.B. Charrier-Savournin, M.T. Chateau, V. Gire, J. Sedivy, J. Piette, V. Dulic, p21-Mediated nuclear retention of cyclin B1-Cdk1 in response to genotoxic stress, Mol. Biol. Cell 15 (2004) 3965–3976.
[48] B.C. Dash, W.S. El-Deiry, Phosphorylation of p21 in G2/M promotes cyclin B-Cdc2 kinase activity, Mol. Cell. Biol. 25 (2005) 3364–3387.

Please cite this article in press as: G. Napolitano, et al., Sequence-specific double strand breaks trigger P-TEFb-dependent Rpb1-CTD hyperphosphorylation, Mutat. Res.: Fundam. Mol. Mech. Mutagen. (2013), http://dx.doi.org/10.1016/j.mrfmmm.2013.07.005